On the derivation of coseismic displacement fields using differential radar interferometry: the Landers earthquake

HOWARD A. ZEBKER AND PAUL ROSEN
Jet Propulsion Laboratory
California Institute of Technology
4800 Oak Grove Drive
Pasadena, CA 9110.9

Tel. (818) *354-8780,* FAX (818) *39>5285,* Email zebker@jakey.jpl.nasa.gov

Introduction

We present a map of the coseismic displacement field resulting from the Landers, CA, June 28, 1992 earthquake derived using data acquired from an orbiting high resolution radar system, We achieve results more accurate than previous space studies and similar in accuracy to those obtained by conventional field survey techniques. Data from the ERS-1 synthetic aperture radar instrument acquired in April, July, and August 1992 are used to generate a high resolution, wide area map of the displacements. The data represent the motion in the direction of the radar line of sight to cm level precision of each 30 m resolution element in a 113 km by 90 km image. Our coseismic displacement contour msrp gives a lobed pattern consistent with theoretical models of the displacement field from the earthquake. Comparison of these data with GPS and EDM survey data yield a correlation of 0.96, thus the radar measurements are a means to extend the point measurements acquired by traditional techniques to an area map format. The technique we use is i) more automatic, ii) more precise, and iii) better validated than previous similar applications of differential radar interferometry. Since we require only remotely-sensed satellite data with no additional requirements for ancillary information, the technique is well suited for global seismic monitoring and analysis.

There has been much recent activity by at least two groups applying the capabilities of radar interferometry to the study of seismic phenomena. Massonet et al. (1993) of Centre National d'Etudes Spatiales (CNES) in Toulouse, France used an interferometric digital elevation model derived from the Europenn Space Agency (ESA) ERS-1 satellite data for analysis of the magnitude 7.3 earthquake centered near Landers, CA on June 28, 1992. In this study a single interferogram which contained phase signals from the local topography and from the earthquake displacements was subtracted from a manipulated USGS 15 minute DEM of the area. The residual phases were interpreted as ground displacements from the event. The interferogram, when corrected for topographic effects, shows a displaced dual-lobed pattern of fringes emanating from the fault zone, where each fringe represents about 2.8 cm of motion in the radar line of sight direction. They also derive a theoretical fringe pattern from a model of the earthquake motion which matches the observations fairly closely.

In this paper, we approach the Landers analysis differently from Massonet et al. by utilizing only data acquired by the ERS- 1 satellite. Our approach overcomes the aforementioned limitations, hence is more readily quantifiable given the radar system parameters, and the quality of the result can be measured "up front." Specifically, imprecision introduced by the USGS DEM in the CNES study is not present, coregistration occurs automatically in forming the interferograms, and the entire usable phase field is "unwrapped," meaning that the displacement at each point is known digitally in an absolute sense. Unwrapping renders the displacement field more amenable to computer modelling and analysis and permits the precision of tbe technique to be increased from the 2.8 cm radar line of sight reported by Massonet to about 0.2 cm obtained here. Further, we verify the accuracy of the measurements by comparing to a displacement field derived from conventional surveying techniques. These survey data were derived from a combination of Electronic Distance Measurement (EDM) lines and Global Positioning System (GPS) satellite receivers. The methods and results presented here can serve as a baseline for the design of a seismic monitoring program.

Summary of theory

A side-looking spaceborne synthetic aperture radar system may map a continuous swath many tens of kilometers in width as the satellite progresses along its orbit track, yielding measurements of the amplitude and phase of radar echoes associated with independent patches on the ground perhaps 10 m in size– this size is the resolution of the radar. We first examine the case where no ground movement between radar observations occurs. Consider two radar systems observing the same ground swath from two positions Al and A2, respectively, as illustrated in Figure 1. The measured phase at each point in each of the two radar images may be taken as equal to the sum of a propagation part proportional to the round-trip distance traveled and a scattering part due to the interaction of the wave with the ground. If each resolution element on the ground behaves the same for each observation (see more on this important condition below), then calculating the difference in the phases removes dependence on the scattering mechanism and gives a quantity dependent only on geometry. If the two path lengths are taken to be ρ and ρ -t $\delta\rho$, the measured phase difference ϕ will be

$$\phi = \frac{4\pi}{\lambda}\delta\rho \tag{1}$$

or 2π times the round-trip distance difference in wavelengths, and

$$\delta\rho \approx B\sin(\theta - a) \tag{2}$$

or

$$6p \approx B_{\parallel}. \tag{3}$$

$B_{\parallel} = B\sin(\theta - \alpha)$ is simply the component of the baseline parallel to the look direction.

Equations (1 - 3) show that the measured phase of an interferometer is the component of the interferometer baseline parallel to the look direction to a given point on the surface *measured* in wavelengths, multiplied by two for round-trip travel. We note that the height sensitivity of the instrument enters through the dependence of the exact look angle O on the altitude z = h – *pcos* θ, where *h* is the height of the sensor above the reference surface.

If a second (denoted prime) interferogram is acquired over the same area, sharing one orbit with the previous pair so that *p* and θ are unchanged (dashed lines in figure 1), we can compare the interferogram phases with each other. This second interferogram is acquired with a different baseline *B'* and baseline orientation o', thus a different $B_{\parallel}'$. Combining (1) and (3) above we obtain

$$\phi' = \frac{4\pi}{\lambda}B_{\parallel}'. \tag{4}$$

Examination of tbe ratio of the two phases yields

$$\frac{\phi}{\phi'} = \frac{B_{\parallel}}{B_{\parallel}'}. \tag{5}$$

In other words the ratio of the phases is equal to the ratio of the parallel components of the baseline, independent of the topography.

Now consider the situation of two interferograms acquired over the same region as before but in this case an earthquake has displaced each resolution element bet ween observations for the primed interferogram. The displacements are assumed small with respect to a resolution cell so that the radar echoes remain correlated. Here in addition to the phase

dependence on topography there is a phase change due to the radar line-of-sight component of the displacement $\Delta\rho$. In this interferogram the phase ϕ' will be given by

$$\phi' = \frac{4\pi}{\lambda}(B_{\parallel}' + \Delta\rho) \quad (6)$$

The displacement term $\Delta\rho$ adds to the topographic phase term, creating confusion in the interpretation of the result. However, if the data from the initial unprimed interferogram are scaled by the ratio of the parallel components of the baseline and subtracted from the primed interferogram, we can obtain a solution dependent only on the displacement of the surface, as follows

$$\phi' - \frac{B_{\parallel}'}{B_{\parallel}} \cdot \phi = \frac{4\pi}{\lambda}\Delta\rho \quad (7)$$

Since the quantity on the left is determined entirely by the phases of the interferograms and the orbit geometries, the line of sight component of the displacement $\Delta\rho$, is measurable for each point in the scene.

ERS-1 Observations of the Landers Earthquake

The ERS-1 radar system, operating at a wavelength of 5.67 cm, images the Earth from an altitude of about 700 km and produces radar backscatter maps of 100 km wide swaths at a resolution of about 25 m across track and 6 m along track. We obtained raw ERS-1 radar signal samples acquired over the Landers region on April 24, July 3, and August 7, 1992. Recombined these to form two interferograms, one from the April-August pair and one from the July-August pair. The April-August pair spans the June 28 earthquake, and was chosen over the April-July pair which exhibited an exceptionally large baseline. No data were acquired on May 29 when the satellite again passed over the site.

We processed the radar signal samples to interferograms at JPL using a software processor constructed specifically by us for ERS-1 interferometric applications. The data were processed using a range-Doppler algorithm, but the range compressed signals were filtered for the July-August pair using the method suggested by Gatelii et al. (1993) to reduce baseline decorrelation. We found that this approach yielded about 5-10 % greater correlation in some regions at the expense of a slight reduction in range resolution.

The interferograms were filtered using a spatially variable bandpass filter that selected the optimal fringe rate passband in each 32 by 32 pixel subregion in the interferogram. In this process we also identified areas of low fringe visibility to serve as a mask in the final product, eliminating regions where we felt we could not trust the phase estimates. The dnta were then unwrapped using the method of Hiramatsu (personal communication, A. Hiramatsu, 1992), which is an extension of the method first presented by Goldstein et al. (1988).

Finally, the differential interferogram was calculated by scaling the July-August measurement by the ratio of the parallel baseline components for each look angle and subtracting that value from the corresponding value in the April-August pair. The result is a map of the displacements of the ground in radar line of sight direction (equation 7). Figure 2 shows the radar reflectivity of the Landers region; in addition, contour lines representing iine of sight displacements spaced every 5 cm are displayed.

Comparison with field measurements

In this section we discuss the accuracy of our measurements and compare the results to those obtained in the field using Global Positioning Satellite (GPS) and Electronic Distance Measurement (EDM) survey data. As a basis of comparison we will use the coseismic displacement field solution as derived by Freymueller et al. (1993), data which were compiled by Hudnut et al. (1993). Hudnut et al. also analyzed these data nnd obtained a slightly different, but consistent solution. These calculated displacements were derived from a combination of GPS data from several sources and EDM line lengths obtained by the USGS (please see the above references for a more detailed description of the data sources and techniques).

As stated previously, the radar technique is sensitive to the line of sight component of motion. We therefore calculated the component of the GPS motion vectors in the direction of the projection on the ground of the radar sensor boresight, the vector from the sensor to a point on the Earth's surface. As for the radar measurements, since the line of sight direction is not in the plane defined by the local Earth surface, we derived the equivalent horizontal surface motion to yield the observed slant range displacement. The results of both of these calculations are shown in figure 3. For each survey site, denoted by a triangle, we illustrate vectors corresponding to motion as (determined by survey techniques (diamond-headed arrows) and as determined by the radar (cross-headed arrows). Note that the radar vectors are all parallel to the edge of the radar image, as only the component of motion in the line of sight is measured. The mean value of the differences is 0.9 cm, and the rms difference is 18.9 cm. The formal correlation of the data is 0.96.

Discussion

We have shown that it is possible to map a coseismic (displacement field resulting from a major earthquake using only data acquired from an orbiting high resolution radar system, and achieve results comparable in magnitude to those obtained by conventional field survey techniques. Data from the ERS-1 synthetic aperture radar instrument acquired at three separate instances of time are sufficient to generate a high resolution, wide area map of the displacements. Comparison of these data with GPS and EDM survey data indicate a high degree of confidence in the radar measurements. We are confident that the differences between the radar and GPS measurements are reconcilable and do not point to a fundamental limitation in the radar technique. Further work is needed along these lines however.

The power of the differential interferometry technique for seismological applications lies in its cm-scale measurement sensitivity of line-of-site displacements over a wide area. The derived displacement fields can be used as a tight constraint in the modeling of earthquake motion. The fine accuracy, fine spatial resolution, and large areal coverage will likely allow increasingly detailed models to be explored, on both large and small spatial scales. The promise of a system to map small scale fractures in the Earth's surface over a wide region automatically with a remote sensing system will greatly facilitate field activities by permitting concentration in the most important areas.

Acknowledgements

We would iike to acknowledge P. Segall for supplying the GPS/EDM measurements and for several useful discussions regarding the intercomparison of the data sets, We would also like to acknowledge discussions with Ken Hudnut for discussions prompting a reexamination of the comparison of our results with the GPS / EDM data. The research described in this paper was carried out by the Jet Propulsion Laboratory, California Institute of Technology, under a contract with the National Aeronautics and Space Administration.

References

Freymueller, J., N.E. King, and P. Segall, The coseismic slip distribution of the Landers earthquake, submitted to *Bull. Seism. Sot.* Am., 1993.

Gatelli, F., A. Monti Guarnieri, F. Parizzi, P. Pasquali, C. Prati, and F, Rocca, Use of the spectral shift in SAR inter ferometry: applications to ERS-1, submitted to *IEEE Trans. on Geosci. and* Rem. *Sens.*, 1993.

Goldstein, R. M., H.A. Zebker, and C.L. Werner, Satellite radar interferometry: two dimensional phase unwrapping, *Radio Science,* 29, 713-720, 1988.

Hudnut, K. W., Y. Bock, M. Cline, P. Fang, Y. Feng, J. Freymueller, X. Ge, W.K. Gross, D. Jackson, M. Kim, N.E. King, S.C. Larsen, M. Lisowski, Z-K. Shen, J. Svarc, and J. Zhang, Coseismic displacements of the 1992 Landers Earthquake Sequence, submitted to *Bull. Seismol.* Sot. *Amer., 1993.*

Massonnet, D., M. Rossi, C. Carmona, F. Adragna, G. Peltzer, K. Feigl, and T. Rabaute, The displacement field of the Landers earthquake mapped by radar interferometry, *Nature, 364,* 133142, 1993.

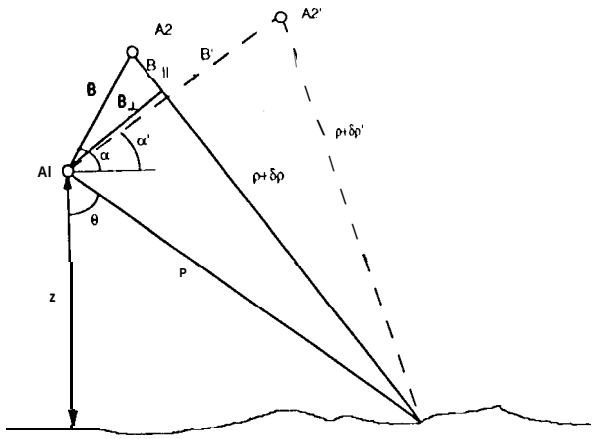

Figure 1. Radar imaging geometry. The solid lines show that radar signal paths for the first interferogram pair formed by antennas at A1 and A2. Dashed lines show signal path for second interferogram acquired over the same site but with antennas located at A 1 and A2'.

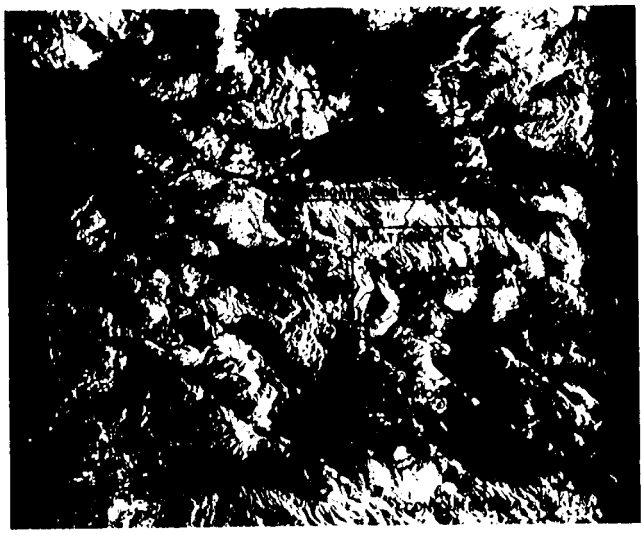

Figure 2. Image of Landers region with the radar reflectivity of the surface shnwn as brightness. Contours indicating each 5 cm of displacement are drawn in black.

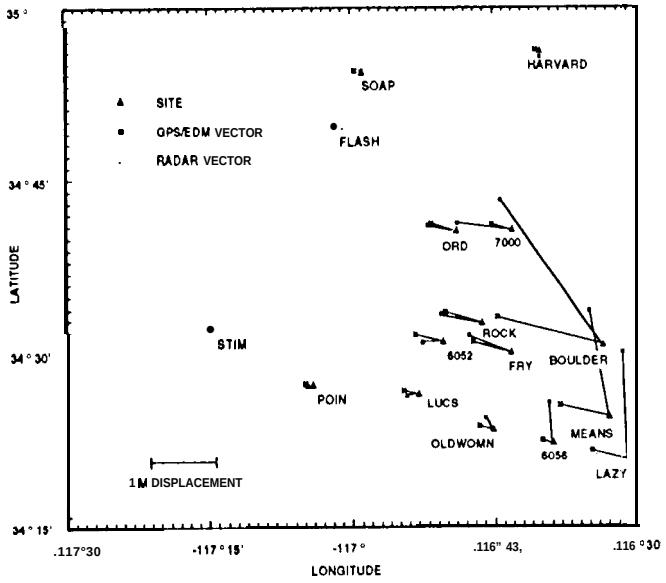

Figure 3. Displacement vectors as measured by GPS/EDM data and by radar interferometry. Each GPS or EDM site is denoted by a triangle, and a vector ending with a square (GPS/EDM measurement) and a vector ending with an 'x' (radar measurement) are shown in the direction of motion. Note that for the radar case only the component in the radar line-of-sight direction is determined and thus all measurements are parallel. Vectors are correlated at 0.96 level and show that radar and field surveys are measuring similar phenomena.